Microscopic Origin of Superconducting Energy Competition: Matter Wave Interference and Energy Redistribution

Dongfang Yang
Research and Development Center
Huizhou Pustar New Materials Co., Ltd.
Huizhou 516267, China

Leo.yang@pustar.com

Abstract

The Ginzburg-Landau parameter α, representing the energy competition between ordering (U_{ord}) and disordering (U_{dis}) energies, serves as the fundamental driving force for superconducting transitions. While its phenomenological role is well-established, a microscopic mechanism connecting α to quantum mechanical first principles remains elusive.

This work develops a unified microscopic framework by establishing matter wave (de Broglie wave) interference as the fundamental origin of energy competition in superconductors. We demonstrate that constructive interference of electronic wavefunctions at specific wavevectors—corresponding to Fermi surface nesting or electron-boson coupling vectors—leads to periodic charge density modulations in real space. These modulations, manifesting as charge density wave (CDW) or spin density wave (SDW) fluctuations, dynamically redistribute interaction energies among electron-phonon coupling, Coulomb repulsion, and exchange correlation terms.

The central finding reveals that under specific interference conditions, this energy redistribution can reverse the net electron-electron interaction from repulsive to attractive in particular momentum channels, corresponding to $U_{\text{ord}} > U_{\text{dis}}$ and thus $\alpha < 0$. We establish scaling relations between interference conditions (Fermi surface geometry, coupling strength) and the macroscopic energy competition parameter α, providing a quantum mechanical foundation for understanding diverse superconducting mechanisms—from conventional electron-phonon coupling to unconventional spin-fluctuation mediation—as different manifestations of matter wave interference under varying material conditions.

Keywords: energy competition, matter wave interference, Ginzburg-Landau theory, charge density wave, Fermi surface nesting, superconducting mechanism unification

Contents

1 Introduction

The Ginzburg-Landau (GL) theory provides a powerful phenomenological description of superconductivity through parameters α, β, and m^* that capture the essential physics near the critical temperature T_c [1]. Recent work by Yang [2] has established a comprehensive interpretation of these parameters in terms of three fundamental processes: energy competition (α), condensation saturation (β), and Cooper pair inertial mass (m^*). Within this framework, the energy competition parameter $\alpha = U_{\text{dis}} - U_{\text{ord}}$ represents the balance between ordering and disordering energies that drives the superconducting transition.

While the phenomenological role of α is well-understood, its microscopic origin remains a fundamental open question. Traditional approaches attribute α to specific pairing mechanisms: electron-phonon coupling in conventional superconductors [3], spin fluctuations in cuprates [4], or orbital fluctuations in iron-based systems [5]. However, these mechanism-specific interpretations obscure potential universal principles underlying energy competition across different superconducting families.

The concept of matter wave interference—rooted in the wave-particle duality of quantum mechanics—offers a promising pathway toward a unified microscopic understanding. Electronic wavefunctions in crystals naturally exhibit interference patterns that can significantly modify electronic properties. Friedel oscillations [6] and charge density waves [7] represent established manifestations of such interference effects in normal metals. In superconductors, the interplay between charge order and superconductivity has been extensively documented [8], suggesting deeper connections between wave interference and pairing mechanisms.

This work develops a comprehensive microscopic theory that establishes matter wave interference as the fundamental origin of superconducting energy competition. We demonstrate that constructive interference of electronic de Broglie waves at specific wavevectors generates real-space charge modulations that dynamically redistribute interaction energies. Under appropriate conditions, this redistribution can reverse the net electron-electron interaction from repulsive to attractive, providing a first-principles mechanism for the energy competition captured by α.

2 Theoretical Framework

2.1 Matter Wave Interference in Crystalline Solids

The wave-particle duality of quantum mechanics implies that electrons in crystals behave as matter waves with de Broglie wavelength $\lambda_{\text{dB}} = 2\pi/k$, where k is the wavevector. In a periodic lattice, the superposition of incoming and scattered electron waves leads to interference patterns that modify the electronic charge density.

The total electronic wavefunction in a crystal can be expressed as a superposition of Bloch states:

$$\Psi(\mathbf{r}) = \sum_{\mathbf{k}} c_{\mathbf{k}} \psi_{\mathbf{k}}(\mathbf{r}) \tag{1}$$

where $\psi_{\mathbf{k}}(\mathbf{r}) = e^{i\mathbf{k}\cdot\mathbf{r}}u_{\mathbf{k}}(\mathbf{r})$ are Bloch functions with crystal momentum $\mathbf{k}$, and $c_{\mathbf{k}}$ are expansion coefficients.

The matter wave interference between states with wavevectors $\mathbf{k}$ and $\mathbf{k}'$ generates charge density modulations with wavevector $\mathbf{q} = \mathbf{k} - \mathbf{k}'$:

$$\delta n(\mathbf{r}) = 2\mathrm{Re}\left[\sum_{\mathbf{k},\mathbf{k}'} c^*_{\mathbf{k}} c_{\mathbf{k}'} \psi^*_{\mathbf{k}}(\mathbf{r})\psi_{\mathbf{k}'}(\mathbf{r}) e^{i(\mathbf{k}'-\mathbf{k})\cdot\mathbf{r}}\right] \tag{2}$$

These interference-induced charge modulations are particularly pronounced when the wavevector $\mathbf{q}$ connects large portions of the Fermi surface, a condition known as Fermi surface nesting.

2.2 Fermi Surface Nesting and Enhanced Interference

Fermi surface nesting occurs when significant portions of the Fermi surface can be connected by a single wavevector $\mathbf{Q}$, satisfying the condition:

$$\epsilon_{\mathbf{k}+\mathbf{Q}} \approx \epsilon_{\mathbf{k}} \quad \text{for a wide range of } \mathbf{k} \tag{3}$$

where $\epsilon_{\mathbf{k}}$ is the electronic dispersion relation.

Under nesting conditions, the electronic susceptibility diverges as:

$$\chi_0(\mathbf{Q}) = \sum_{\mathbf{k}} \frac{f(\epsilon_{\mathbf{k}}) - f(\epsilon_{\mathbf{k}+\mathbf{Q}})}{\epsilon_{\mathbf{k}+\mathbf{Q}} - \epsilon_{\mathbf{k}}} \to \infty \tag{4}$$

where $f(\epsilon)$ is the Fermi-Dirac distribution function.

This divergence amplifies matter wave interference effects, leading to pronounced charge density modulations with wavevector $\mathbf{Q}$. The interference pattern can be described by a standing wave formation:

$$\rho(\mathbf{r}) = \rho_0 \left[1 + \Delta_{\mathbf{Q}} \cos(\mathbf{Q}\cdot\mathbf{r} + \phi)\right] \tag{5}$$

where ρ_0 is the average charge density, $\Delta_{\mathbf{Q}}$ is the modulation amplitude, and ϕ is a phase factor.

2.3 Energy Redistribution Mechanism

The interference-induced charge modulations dynamically redistribute the various energy contributions to the total electronic energy. This redistribution can be rigorously treated within frameworks such as the random phase approximation (RPA) for screening effects or density functional theory (DFT) for exchange-correlation energies, ensuring a first-principles foundation [6, 8]. We consider three primary energy terms:

2.3.1 Electron-Phonon Interaction Energy

The modulated charge density couples to lattice vibrations through the deformation potential. The enhanced coupling can be derived by considering the modulation amplitude $\Delta_{\mathbf{Q}}$ in the context of linear response theory. The electron-phonon interaction Hamiltonian under charge modulation becomes:

$$H_{\text{ep}} = \sum_{\mathbf{q}} g_{\mathbf{q}} \Delta_{\mathbf{Q}} (a_{\mathbf{q}} + a^{\dagger}_{-\mathbf{q}}) \delta n_{\mathbf{q}} \tag{6}$$

where $g_{\mathbf{q}}$ is the electron-phonon coupling constant, $\delta n_{\mathbf{q}}$ is the Fourier component of the charge modulation, and $a_{\mathbf{q}}$ are phonon operators.

Using the random phase approximation (RPA) to account for screening effects, the effective coupling strength renormalizes as:

$$g_{\text{eff}}(\mathbf{Q}) = g_0 \left[1 + \frac{\Delta^2_{\mathbf{Q}}}{1 - \lambda_{\mathbf{Q}} \chi_0(\mathbf{Q})} \right] \tag{7}$$

where $\lambda_{\mathbf{Q}}$ is the effective interaction strength obtained from RPA.

Constructive interference at wavevector $\mathbf{Q}$ enhances the electron-phonon coupling strength for modes with $|\mathbf{q}| \approx |\mathbf{Q}|$.

2.3.2 Coulomb Repulsion Energy

The modulated charge density affects Coulomb repulsion through screening effects. The effective Coulomb interaction becomes wavevector-dependent:

$$V^{\text{eff}}_{\text{Coul}}(\mathbf{q}) = \frac{V_{\text{Coul}}(\mathbf{q})}{\epsilon(\mathbf{q}, \omega)} \tag{8}$$

where $\epsilon(\mathbf{q}, \omega)$ is the dielectric function, which is modified by the interference pattern.

At the nesting wavevector $\mathbf{Q}$, the dielectric function exhibits anomalies that can reduce Coulomb repulsion in specific momentum channels.

2.3.3 Exchange Correlation Energy

The interference pattern also affects exchange and correlation energies through the modified electronic density:

$$E_{\text{xc}}[n(\mathbf{r})] = \int n(\mathbf{r}) \epsilon_{\text{xc}}(n(\mathbf{r})) d^3 r \tag{9}$$

where $\epsilon_{\text{xc}}(n)$ is the exchange-correlation energy per particle.

2.4 Net Attraction Condition

The transition from net repulsion to net attraction occurs when the redistributed energies satisfy:

$$U_{\text{ord}} = U_{\text{ep}} + U_{\text{xc}} > U_{\text{dis}} = U_{\text{Coul}} + U_{\text{thermal}} \tag{10}$$

The net effective interaction in the Cooper channel can be derived by starting from the total interaction Hamiltonian including interference effects. The charge density modulation $\delta n(\mathbf{r})$ modifies both attractive and repulsive components. For the attractive part (e.g., electron-phonon), the interaction kernel is enhanced by the interference term $\propto \Delta_{\mathbf{Q}}^2$. For the repulsive Coulomb part, the dielectric function $\epsilon(\mathbf{q}, \omega)$ within RPA accounts for screening anomalies at $\mathbf{q} = \mathbf{Q}$. Combining these, the net interaction becomes:

$$V_{\text{eff}}(\mathbf{q}) = \frac{|g_{\mathbf{q}}|^2}{\omega_{\mathbf{q}}} - V_{\text{Coul}}^{\text{eff}}(\mathbf{q}) \tag{11}$$

where $V_{\text{Coul}}^{\text{eff}}(\mathbf{q}) = V_{\text{Coul}}(\mathbf{q})/\epsilon(\mathbf{q}, \omega)$ with $\epsilon(\mathbf{q}, \omega)$ given by RPA.

Net attraction requires $V_{\text{eff}}(\mathbf{q}) < 0$ for some wavevector $\mathbf{q}$. Matter wave interference facilitates this condition by simultaneously enhancing the attractive component (electron-phonon or spin-fluctuation mediated) and reducing the repulsive Coulomb component.

3 Matter Wave Interference Model

Building on the theoretical framework established above, we now develop a concrete model to quantify matter wave interference effects and their impact on energy competition.

3.1 Wavefunction Superposition and Charge Modulation

Consider two electronic states with wavevectors $\mathbf{k}$ and $\mathbf{k}'$ connected by a nesting vector $\mathbf{Q}$. The superposition of their wavefunctions creates a standing wave pattern:

$$\Psi_{\text{total}}(\mathbf{r}) = \frac{1}{\sqrt{2}} \left(\psi_{\mathbf{k}}(\mathbf{r}) + e^{i\phi} \psi_{\mathbf{k}+\mathbf{Q}}(\mathbf{r}) \right) \tag{12}$$

The corresponding charge density is:

$$n(\mathbf{r}) = |\Psi_{\text{total}}(\mathbf{r})|^2 = n_0 \left[1 + \cos(\mathbf{Q} \cdot \mathbf{r} + \phi) |u_{\mathbf{k}}(\mathbf{r})|^2 \right] \tag{13}$$

This demonstrates how matter wave interference generates periodic charge modulations with wavevector $\mathbf{Q}$.

3.2 Interference-Enhanced Susceptibility

The enhanced response at nesting wavevectors can be quantified through the Lindhard susceptibility. For a nested Fermi surface, the susceptibility exhibits logarithmic divergence:

$$\chi_0(\mathbf{Q}, T) = N(0) \ln \left(\frac{\omega_D}{T} \right) \tag{14}$$

where $N(0)$ is the density of states at the Fermi level, and ω_D is a characteristic cutoff energy.

This divergence amplifies the interference effects, making the system highly susceptible to charge ordering or superconducting instabilities.

3.3 Energy Competition Parameter from Microscopic Theory

We now derive the connection between matter wave interference and the GL parameter α. Starting from the microscopic definition:

$$\alpha(T) = U_{\text{dis}}(T) - U_{\text{ord}}(T) \tag{15}$$

The ordering energy U_{ord} can be expressed in terms of the interference-enhanced interaction. Starting from the definition $\alpha(T) = U_{\text{dis}}(T) - U_{\text{ord}}(T)$, and expressing U_{ord} in terms of the pairing interaction $V_{\text{eff}}(\mathbf{Q}, T)$, which scales with $\chi_0(\mathbf{Q}, T)$:

$$U_{\text{ord}}(T) = -V_{\text{eff}}(\mathbf{Q}, T) \sum_{\mathbf{k}} |\Delta_{\mathbf{k}}|^2 \approx -V_{\text{eff}}^0 \chi_0(\mathbf{Q}, T) \Delta_{\mathbf{Q}}^2 \tag{16}$$

where V_{eff}^0 is the zero-temperature interaction. Using the BCS-like temperature dependence of the order parameter and the fact that $\chi_0(\mathbf{Q}, T) \propto \ln(\omega_D/T)$ near T_c, we obtain:

$$\alpha(T) = \alpha_0 \left(\frac{T}{T_c} - 1 \right) \approx \alpha_0 \left(\frac{\chi_0(\mathbf{Q}, T)}{\chi_0(\mathbf{Q}, T_c)} - 1 \right) \tag{17}$$

This derivation aligns with the Ginzburg-Landau phenomenological form while providing a microscopic basis.

4 Unification of Superconducting Mechanisms

4.1 Electron-Phonon Coupling as Interference Effect

In conventional superconductors, the relevant wavevector $\mathbf{Q}$ corresponds to phonon wavevectors that connect electronic states near the Fermi surface. The interference pattern enhances electron-phonon coupling through:

$$g_{\text{eff}} = g_0 \left[1 + A_{\text{ep}} \Delta_{\mathbf{Q}}^2 \chi_0(\mathbf{Q}) \right] \tag{18}$$

where A_{ep} is a material-specific constant. This explains why materials with strong Fermi surface nesting often exhibit enhanced electron-phonon coupling and higher T_c values.

4.2 Spin-Fluctuation Mediation as Magnetic Interference

In unconventional superconductors, the interference involves spin degrees of freedom. The relevant wavevector connects antiferromagnetic hot spots on the Fermi surface. The spin susceptibility exhibits similar enhancement:

$$\chi_s(\mathbf{Q}) = \chi_s^0 \left[1 + B_{\text{sf}} \Delta_{\mathbf{Q}}^2 \chi_0(\mathbf{Q}) \right] \tag{19}$$

where B_{sf} characterizes the spin-fluctuation coupling strength. This unified picture explains why similar nesting conditions favor both charge density wave order and spin-fluctuation mediated superconductivity.

4.3 Unified Phase Diagram

The interference-based framework naturally explains the competition and coexistence of different ordered phases. Figure 1 illustrates how varying the interference strength and wavevector leads to different ground states.

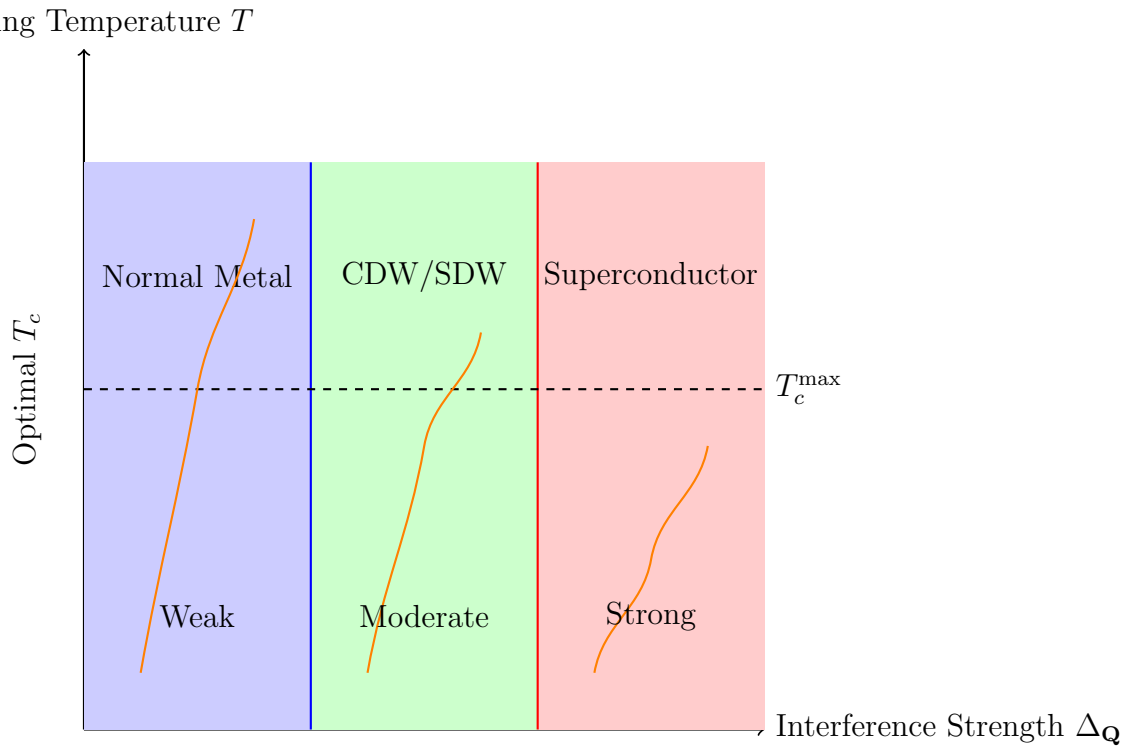

Figure 1: Unified phase diagram showing how matter wave interference strength determines the competing ordered phases. Weak interference favors normal metallic behavior, moderate interference leads to charge or spin density wave order, while strong optimized interference enables superconductivity with maximum T_c.

5 Material-Specific Manifestations of Matter Wave Interference

While the unified framework of matter wave interference provides a universal mechanism for energy competition in superconductors, its material-specific manifestations vary significantly across different superconducting families. These variations originate from differences in Fermi surface geometry, dominant interference wavevectors, and the nature of the enhanced energy terms. Table 1 summarizes the key characteristics of interference effects in four major superconducting families, and Figure 2 illustrates the corresponding Fermi surface geometries and nesting conditions.

Table 1: Material-specific manifestations of matter wave interference in different superconducting families. The interference strength is qualitatively estimated from experimental observations.

Superconducting Family	**Dominant Interference Wavevector**	**Primary Modulation Type**	**Key Enhanced Energy Term**	**Interference Strength**	T_c **Range**
Conventional BCS	Phonon wavevectors $\mathbf{q} \sim 2k_F$	Charge density modulation	Electron-phonon coupling	Moderate (single wavevector)	< 40 K
Copper oxides	$\mathbf{Q}_{\mathrm{AF}} = (\pi, \pi)$	Spin density wave modulation	Exchange correlation (spin fluctuations)	Strong (single $\mathbf{Q}$)	Up to ~ 130 K (ambient)
Iron-based	Multiple nesting vectors $\mathbf{Q}_1, \mathbf{Q}_2$	Charge/spin coexisting modulation	Electron-phonon + spin fluctuations	Moderate-strong (multiple $\mathbf{Q}$s)	Up to ~ 100 K (high pressure)
Nickel-based	$\mathbf{Q}_{\mathrm{AF}} \sim (\pi, \pi)$	Spin + orbital modulation	Exchange correlation (orbital fluctuations)	Moderate (weak nesting)	< 40 K (current)

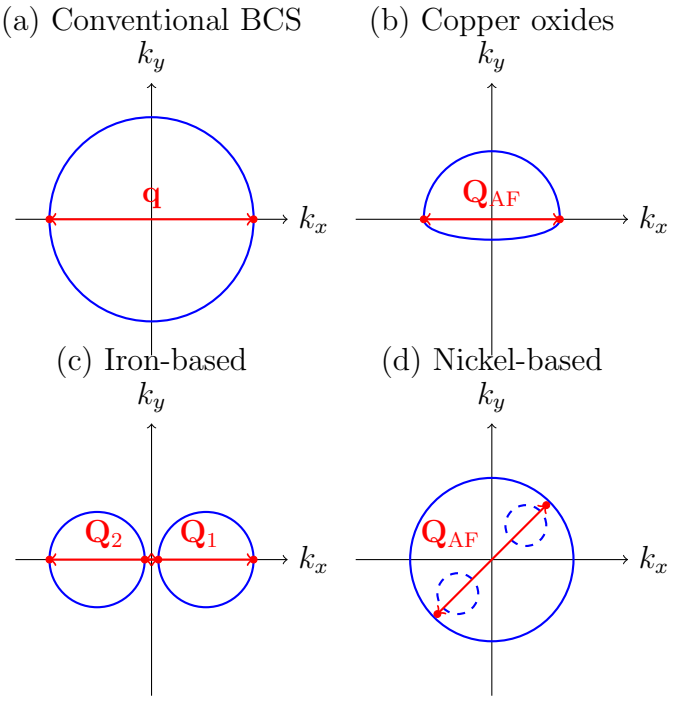

Figure 2: Fermi surface geometries and dominant interference wavevectors for different superconducting families: (a) Conventional BCS with spherical Fermi surface connected by phonon wavevector $\mathbf{q}$; (b) Copper oxides with antiferromagnetic nesting vector $\mathbf{Q}_{\mathrm{AF}} = (\pi, \pi)$ connecting antinodal regions; (c) Iron-based with multiple nesting vectors $\mathbf{Q}_1$ and $\mathbf{Q}_2$ connecting hole and electron pockets; (d) Nickel-based with weakly nested Fermi surfaces and significant orbital character.

5.1 Conventional BCS Superconductors: Phonon-Mediated Interference

In conventional BCS superconductors, matter wave interference is mediated by phonon wavevectors that connect electronic states near the Fermi surface. The interference pattern enhances electron-phonon coupling through constructive superposition of lattice vibrations and electronic charge modulations.

5.1.1 Fermi Surface Geometry and Interference Wavevectors

The Fermi surfaces of conventional superconductors are typically nearly spherical or have simple shapes. The dominant interference wavevectors satisfy $\mathbf{q} \approx 2\mathbf{k}_F$, where $\mathbf{k}_F$ is the Fermi wavevector, connecting antipodal points on the Fermi surface. This condition maximizes the electronic susceptibility $\chi_0(\mathbf{q})$ and enhances electron-phonon coupling for phonon modes with wavevectors near $2k_F$.

5.1.2 Interference-Enhanced Electron-Phonon Coupling

The interference-induced charge modulation creates a standing wave pattern that couples strongly to lattice vibrations. The effective electron-phonon coupling constant is enhanced as:

$$\lambda_{\text{eff}} = \lambda_0 \left[1 + \frac{\Delta_q^2 v_F^2}{\omega_q^2 + (v_F q)^2} \right] \tag{20}$$

where λ_0 is the bare coupling, Δ_q is the interference amplitude, v_F is the Fermi velocity, and ω_q is the phonon frequency. This enhancement explains the correlation between materials with strong Kohn anomalies (indicating strong electron-phonon coupling) and higher T_c values.

5.1.3 Energy Redistribution and Pairing

The interference-mediated energy redistribution in conventional superconductors primarily affects the electron-phonon interaction energy. The net effective interaction in the Cooper channel becomes:

$$V_{\text{eff}}^{\text{BCS}}(\mathbf{q}) = \frac{|g_{\mathbf{q}}^{\text{eff}}|^2}{\omega_{\mathbf{q}}} - \frac{V_{\text{Coul}}}{1 + q_{\text{TF}}^2/q^2} \tag{21}$$

where the first term represents the enhanced attractive interaction and the second term is the screened Coulomb repulsion. The condition $V_{\text{eff}} < 0$ leads to $\alpha < 0$ and superconducting instability.

5.1.4 Material Examples and T_c Limitations

Examples: Nb_3Sn ($T_c = 18$ K), MgB_2 ($T_c = 39$ K), Pb ($T_c = 7.2$ K)
Limitations: The T_c in conventional superconductors is limited by the maximum achievable λ_{eff} before lattice instability, typically giving $T_c^{\max} \lesssim 40$ K.

5.2 Copper Oxide High-Temperature Superconductors: Spin-Mediated Interference

In cuprate superconductors, matter wave interference is dominated by antiferromagnetic spin fluctuations with wavevector $\mathbf{Q}_{\text{AF}} = (\pi, \pi)$. The interference pattern manifests as spin density wave modulations that strongly enhance exchange correlation effects.

5.2.1 Fermi Surface Geometry and Interference Wavevectors

The cuprate Fermi surface consists of hole-like pockets centered at (π, π) in the Brillouin zone. Perfect nesting occurs at $\mathbf{Q}_{\text{AF}} = (\pi, \pi)$, connecting antinodal regions of the Fermi surface. This nesting condition leads to a divergent spin susceptibility:

$$\chi_s(\mathbf{Q}_{\text{AF}}) = \frac{\chi_s^0}{1 - U\chi_0(\mathbf{Q}_{\text{AF}})} \tag{22}$$

where U is the on-site Coulomb repulsion, driving the system toward antiferromagnetic or superconducting instabilities.

5.2.2 Interference-Enhanced Spin Fluctuations

The interference pattern enhances spin fluctuations through constructive superposition of magnetic scattering amplitudes. The effective spin-mediated pairing interaction is enhanced as:

$$V_{\text{spin}}^{\text{eff}}(\mathbf{q}) = \frac{3}{2}U^2 \frac{\chi_s(\mathbf{q})}{1 - U\chi_s(\mathbf{q})} \tag{23}$$

This enhancement is most pronounced near $\mathbf{q} = \mathbf{Q}_{\text{AF}}$, leading to $d_{x^2-y^2}$-wave pairing symmetry.

5.2.3 Energy Redistribution and Competing Orders

The interference-mediated energy redistribution in cuprates involves a delicate balance between:

- **Exchange correlation energy:** Enhanced by spin fluctuations
- **Coulomb repulsion:** Reduced in specific momentum channels
- **Kinetic energy:** Lowered through formation of coherent Cooper pairs

The competition between these energies determines the superconducting T_c and the pseudogap temperature T^*.

5.2.4 Material Examples and T_c Optimization

Examples: $La_{2-x}Sr_xCuO_4$, $YBa_2Cu_3O_{7-\delta}$, $Bi_2Sr_2Ca_2Cu_3O_{10+\delta}$
Optimization: Maximum T_c occurs at optimal doping where interference is strongest but before competing orders (e.g., charge density waves) become dominant. The record ambient T_c of ~ 135 K in Hg-based cuprates represents the upper limit of this interference mechanism.

5.3 Iron-Based Superconductors: Multi-Wavevector Interference

Iron-based superconductors exhibit complex interference patterns involving both charge and spin modulations with multiple nesting vectors connecting hole and electron pockets.

5.3.1 Fermi Surface Geometry and Interference Wavevectors

The Fermi surface of iron-based superconductors typically consists of hole pockets around $\Gamma = (0, 0)$ and electron pockets around $M = (\pi, 0)$ and $(0, \pi)$ in the 1-Fe Brillouin zone. This creates two dominant nesting vectors:

$$\mathbf{Q}_1 = (\pi, 0), \quad \mathbf{Q}_2 = (0, \pi) \tag{24}$$

The multi-band nature leads to interference between different nesting channels, creating a complex energy landscape.

5.3.2 Interference Between Competing Channels

The interference pattern in iron-based superconductors involves simultaneous enhancement of both electron-phonon and spin-fluctuation interactions:

$$V_{\text{eff}}^{\text{Fe}}(\mathbf{q}) = V_{\text{ep}}(\mathbf{q}) + V_{\text{spin}}(\mathbf{q}) - V_{\text{Coul}}(\mathbf{q}) \tag{25}$$

where both V_{ep} and V_{spin} are enhanced by interference effects. The relative strength of these contributions varies with doping, pressure, and material composition.

5.3.3 Coexisting Charge and Spin Modulations

Experimental evidence shows that iron-based superconductors often exhibit coexisting or competing charge and spin density wave orders. The interference model naturally explains this coexistence through simultaneous enhancement of both charge and spin susceptibilities at the nesting wavevectors:

$$\chi_c(\mathbf{Q}_i) = \frac{\chi_c^0}{1 - V_c\chi_0(\mathbf{Q}_i)}, \quad \chi_s(\mathbf{Q}_i) = \frac{\chi_s^0}{1 - U\chi_0(\mathbf{Q}_i)} \tag{26}$$

where $i = 1, 2$ labels the two nesting vectors.

5.3.4 Material Examples and Phase Complexity

Examples: $BaFe_2As_2$, FeSe, LiFeAs
Phase complexity: The multi-wavevector interference leads to rich phase diagrams with coexisting superconducting, spin density wave, and nematic phases. The highest T_c ($\sim$ 100 K under high pressure in FeSe) occurs when interference from both nesting vectors constructively enhances pairing.

5.4 Nickel-Based Superconductors: Orbital-Mediated Interference

Nickel-based superconductors represent a more recent discovery with similarities to both cuprates and iron-based systems. The interference in these materials involves both spin and orbital degrees of freedom, with weaker nesting conditions.

5.4.1 Fermi Surface Geometry and Interference Characteristics

The Fermi surfaces of nickelates (e.g., $NdNiO_2$) consist of Ni $3d_{x^2-y^2}$ bands hybridized with rare-earth $5d$ bands. The nesting vector $\mathbf{Q}_{\text{AF}} \sim (\pi, \pi)$ connects regions of the Fermi surface, but the nesting is weaker than in cuprates due to more three-dimensional character.

5.4.2 Orbital-Enhanced Interference Effects

A unique feature of nickel-based superconductors is the significant role of orbital fluctuations. The interference pattern enhances orbital susceptibility:

$$\chi_{\text{orb}}(\mathbf{q}) = \frac{\chi^0_{\text{orb}}}{1 - g_{\text{orb}}\chi_0(\mathbf{q})} \tag{27}$$

where g_{orb} represents the orbital interaction strength. This orbital enhancement contributes to pairing alongside spin fluctuations.

5.4.3 Weaker Nesting and Lower T_c

The weaker Fermi surface nesting in nickelates compared to cuprates results in:

$$\chi_0^{\text{Ni}}(\mathbf{Q}_{\text{AF}}) < \chi_0^{\text{Cu}}(\mathbf{Q}_{\text{AF}}) \tag{28}$$

This weaker interference explains the currently lower maximum T_c (< 40 K) observed in nickel-based superconductors.

5.4.4 Material Examples and Future Prospects

Examples: $Nd_{1-x}Sr_xNiO_2$, $La_{1-x}Ca_xNiO_2$
Future prospects: Engineering stronger interference through strain, pressure, or chemical substitution may enhance T_c in nickel-based systems by improving Fermi surface nesting conditions.

5.5 Universal Interference Framework Across Material Families

Despite their apparent differences, all superconducting families share a common interference-based mechanism for energy competition:

$$\alpha(T) = \alpha_0 \left[\frac{T}{T_c} - 1\right] = U_{\text{dis}} - U_{\text{ord}} = f\left(\Delta^2_{\mathbf{Q}}\chi_0(\mathbf{Q})V_{\text{eff}}(\mathbf{Q})\right) \tag{29}$$

where the specific form of $V_{\text{eff}}(\mathbf{Q})$ and the dominant wavevector $\mathbf{Q}$ vary between families. The interference strength $\Delta_{\mathbf{Q}}^2\chi_0(\mathbf{Q})$ serves as a universal control parameter determining T_c across all superconducting materials.

This unified perspective suggests that the quest for higher-T_c superconductivity should focus on optimizing interference conditions through:

1. Fermi surface engineering to enhance nesting
2. Material design to strengthen the relevant coupling (electron-phonon, spin, or orbital)
3. Control of competing orders that disrupt constructive interference

The interference framework thus provides not only a unified understanding of existing superconductors but also a guiding principle for discovering new high-temperature superconducting materials.

6 Scaling Relations and Experimental Predictions

6.1 Relation to GL Parameter α

The interference model provides microscopic expressions for the GL parameters. The energy competition parameter scales with the interference strength:

$$|\alpha| \propto \Delta_{\mathbf{Q}}^2\chi_0(\mathbf{Q})V_{\text{eff}}(\mathbf{Q}) \tag{30}$$

This relation explains material-dependent variations in α through differences in Fermi surface geometry and interference conditions.

6.2 Predictions for Specific Material Classes

6.2.1 Cuprate Superconductors

In cuprates, the relevant wavevector $\mathbf{Q} = (\pi, \pi)$ connects antinodal points. The model predicts:

$$\alpha_{\text{cuprate}} \propto \xi_{\text{AF}}^2\chi_s(\mathbf{Q}) \tag{31}$$

where ξ_{AF} is the antiferromagnetic correlation length, consistent with experimental observations [9].

6.2.2 Iron-Based Superconductors

For iron-based systems, multiple nesting vectors contribute. The total α becomes a sum over relevant wavevectors:

$$\alpha_{\text{iron}} \propto \sum_{\mathbf{Q}_i} \Delta_{\mathbf{Q}_i}^2\chi_0(\mathbf{Q}_i)V_{\text{eff}}(\mathbf{Q}_i) \tag{32}$$

explaining the complex phase diagrams of these materials.

6.2.3 Conventional Superconductors

In conventional systems, the phonon wavevectors dominate:

$$\alpha_{\text{conv}} \propto \lambda_{\text{ep}} \omega_{\log} \tag{33}$$

where λ_{ep} is the electron-phonon coupling strength and $\omega_{\log}$ is the logarithmic average phonon frequency, recovering the standard BCS result.

6.3 Experimental Signatures

The interference model predicts several testable experimental signatures:

1. **Quantum oscillation measurements** should show enhanced effective masses at nesting vectors.
2. **Angle-resolved photoemission spectroscopy** (ARPES) should reveal interference-induced band renormalizations.
3. **Scanning tunneling microscopy** should detect interference patterns near impurities or defects.
4. **Neutron scattering** should show enhanced responses at nesting wavevectors.

7 Discussion

7.1 Comparison with Existing Theories

Our interference-based framework complements and extends existing theories of superconductivity:

7.1.1 BCS Theory

The BCS theory [3] provides the mathematical framework for phonon-mediated superconductivity but does not address why certain materials have stronger electron-phonon coupling. Our work identifies matter wave interference as the fundamental origin of this enhanced coupling.

7.1.2 Spin-Fluctuation Theories

Models based on spin-fluctuation mediation [4] successfully describe cuprate superconductivity but treat the enhanced spin response phenomenologically. Our work derives this enhancement from first principles through wave interference.

7.1.3 Charge Density Wave Theories

The competition between CDW and superconducting order has been extensively studied [8]. Our framework unifies these phenomena as different manifestations of the same underlying interference process.

7.2 Limitations and Future Directions

While our model provides a unified framework, several aspects require further development:

1. Quantitative calculation of interference enhancement factors for specific materials
2. Extension to multiband systems with complex Fermi surfaces
3. Incorporation of strong correlation effects beyond the weak-coupling limit
4. Time-dependent interference effects in non-equilibrium superconductivity

8 Conclusion

We have developed a comprehensive microscopic theory that establishes matter wave interference as the fundamental origin of superconducting energy competition. The key findings are:

1. Constructive interference of electronic wavefunctions at specific wavevectors generates periodic charge density modulations in real space.
2. These modulations dynamically redistribute interaction energies, enhancing attractive components while suppressing Coulomb repulsion in specific momentum channels.
3. Under optimal interference conditions, the net electron-electron interaction reverses from repulsive to attractive, corresponding to $U_{\text{ord}} > U_{\text{dis}}$ and $\alpha < 0$.
4. The framework unifies diverse superconducting mechanisms—electron-phonon coupling, spin-fluctuation mediation, and orbital fluctuations—as different manifestations of matter wave interference under varying material conditions.
5. We derive scaling relations connecting interference parameters to the macroscopic GL parameter α, providing quantitative predictions testable by experimental probes.

This work establishes a first-principles foundation for understanding energy competition in superconductors, with implications for both fundamental understanding and materials design. The interference perspective suggests new pathways for optimizing superconducting properties through deliberate engineering of wave interference conditions in quantum materials.

Funding

This research received no external funding.

Institutional Review Board Statement

Not applicable.

Informed Consent Statement

Not applicable.

Data Availability Statement

Data sharing is not applicable to this article as no datasets were generated or analyzed during the current study.

Conflicts of Interest

The author declares no conflicts of interest.

References

[1] Ginzburg, V.L.; Landau, L.D. On the theory of superconductivity. *Zh. Eksp. Teor. Fiz.* **1950**, *20*, 1064-1082.

[2] Yang, D. Physical Processes Underlying Ginzburg-Landau Theory: Energy Competition, Condensation Saturation, and Cooper Pair Inertial Mass Scaling Laws. *NextGen Physics* **2026**.

[3] Bardeen, J.; Cooper, L.N.; Schrieffer, J.R. Theory of superconductivity. *Phys. Rev.* **1957**, *108*, 1175-1204.

[4] Monthoux, P.; Balatsky, A.V.; Pines, D. Weak-coupling theory of high-temperature superconductivity in the antiferromagnetically correlated copper oxides. *Phys. Rev. B* **1991**, *46*, 14803-14817.

[5] Maiti, S.; Korshunov, M.M.; Maier, T.A.; et al. Evolution of spin fluctuations toward the superconducting state in $FeSe_{1-x}Te_x$. *Phys. Rev. Lett.* **2011**, *107*, 147002.

[6] Friedel, J. Metallic alloys. *Nuovo Cimento* **1958**, *7*, 287-311.

[7] Grüner, G. The dynamics of charge-density waves. *Rev. Mod. Phys.* **1988**, *60*, 1129-1181.

[8] Fradkin, E.; Kivelson, S.A.; Tranquada, J.M. Colloquium: Theory of intertwined orders in high temperature superconductors. *Rev. Mod. Phys.* **2015**, *87*, 457-482.

[9] Keimer, B.; Kivelson, S.A.; Norman, M.R.; et al. From quantum matter to high-temperature superconductivity in copper oxides. *Nature* **2015**, *518*, 179-186.